ACTIVE 2006
18-20 SEPTEMBER 2006
ADELAIDE AUSTRALIA

A high-authority/low-authority control strategy for coupled aircraft-style bays

N. H. Schiller[a], C. R. Fuller
Virginia Tech
Blacksburg, VA
United States, 24061

R. H. Cabell
NASA Langley Research Center
Hampton, VA
United States, 23681

ABSTRACT

This paper presents a numerical investigation of an active structural acoustic control strategy for coupled aircraft-style bays. While structural coupling can destabilize or limit the performance of some model-based decentralized control systems, fully-coupled centralized control strategies are impractical for typical aircraft containing several hundred bays. An alternative is to use classical rate feedback with matched, collocated transducer pairs to achieve active damping. Unfortunately, due to the conservative nature of this strategy, stability is guaranteed at the expense of achievable noise reduction. Therefore, this paper describes the development of a combined control strategy using robust active damping in addition to a high-authority controller based on linear quadratic Gaussian (LQG) theory. The combined control system is evaluated on a tensioned, two-bay model using piezoceramic actuators and ideal point velocity sensors. Transducer placement on the two-bay structure is discussed, and the advantages of a combined control strategy are presented.

1 INTRODUCTION

Active control strategies designed to reduce turbulent boundary layer (TBL) induced noise in commercial and general aviation aircraft have received a lot of attention in the past decade. Since boundary layer noise is essentially random in space and time, a coherent reference signal is often unavailable. Therefore, a common approach is to feed back signals from accelerometers or piezoelectric transducers to piezoceramic actuators integrated in the structure [1]. One particularly simple and robust control strategy uses a distributed array of actuator/sensor pairs with local feedback loops, as described by Elliott et al. [2]. If the transducer pairs are collocated and dual, then any passive (energy dissipative) control law, such as negative rate feedback, will guarantee unconditional stability of the closed-loop system [3]. Unfortunately, real transducer pairs are never perfectly collocated and dual, which eliminates the passive property of the system at high frequencies. Despite this limitation, researchers have shown promising results using real transducer pairs [4, 5, 6]. Since this approach essentially augments the inherent damping in the structure, it is well suited for lightly damped metallic structures such as the aluminum sidewall of an aircraft. However, the conservative nature of this technique provides the stability guarantees at the expense of performance. Therefore, it has been referred to as a low-authority control (LAC) approach [7].

In contrast, high-authority control (HAC) approaches offer potential performance benefits, as shown by Clark and Cox [8], at the expense of controller robustness. Since HAC approaches, such as linear quadratic Gaussian (LQG) control, are model based, the performance of the controller depends on the fidelity of the model [9]. Poorly modeled dynamics can cause spillover or destabilize the closed-loop system. Spillover is the unde-

[a]Email address: nschille@vt.edu

sired amplification of the response with respect to the open-loop system. Despite this limitation, researchers have experimentally shown that HAC approaches can be used effectively to reduce the radiated sound power from simple structures [10, 11, 12]. Unfortunately, transitioning decentralized HAC systems from single bay structures to more realistic multiple-bay structures is difficult, as explained by Gibbs and Cabell [13]. Although a fully-coupled, centralized control strategy avoids some of the problems associated with decentralized control, it is not practical for large multiple-bay systems. Since the goal of this work is to develop a control system that can be scaled up with little additional complexity, centralized control strategies are not discussed in this paper.

A high-authority/low-authority control (HAC/LAC) architecture, originally developed to control large flexible space structures, can be used to combine the robustness benefits of collocated rate feedback with the performance benefits of modern control strategies [7, 14, 15, 16]. The HAC portion of the controller is typically designed to meet the performance objective, while the LAC loops add damping and reduce the spillover problems associated with HAC of lightly damped systems.

A combined HAC/LAC strategy designed to reduce the sound radiation from aircraft-style panels could be particularly beneficial if a partially correlated and causal reference signal was available. While TBL noise is essentially random in space and time, a component of jet noise called shockcell noise is spatially correlated with a broad spectral peak [17]. If a reference signal correlated with shockcell noise was available, then a feedforward high-authority approach could be combined with low-authority local feedback loops. This type of combined control system could provide overall performance benefits for mixed disturbances, such as TBL and shockcell noise.

However, for this paper we assume that no reference signal is available, and present a combined control strategy using LQG control and active damping. The paper begins with a description of the coupled two-bay model used for these simulations. Next, results are presented for a decentralized LQG system, along with some of the advantages and disadvantages of that approach. Three LAC configurations are then discussed, followed by the combined HAC/LAC system.

2 SYSTEM STUDIED

This analysis considers a thin aluminum panel, $508\,\text{mm} \times 536\,\text{mm} \times 1.6\,\text{mm}$, partitioned into two bays by a stiffener, as shown in Figure 1. The panel represents a section of an aircraft's fuselage, which is set between rigid ring frames and stiffened by a stringer. For this analysis, the stiffener is offset from the middle of the panel by 11 mm to make the two bays different sizes. In addition, all edges of the stiffened panel are assumed to be clamped, and in-plane tension is included to simulate the hoop stress in a pressurized fuselage.

Analytical models of relatively simple stiffened panels can be created using transfer matrix or finite element-strip methods [18, 19]. These techniques have been used to analyze two-dimensional structures when the eigenfunctions in one direction are already known. A more general approach is to perform a normal modes analysis of the structure using numerical finite element methods. For this work, a finite element model of the stiffened panel was created using MSC.NASTRAN. A normal modes analysis was then used

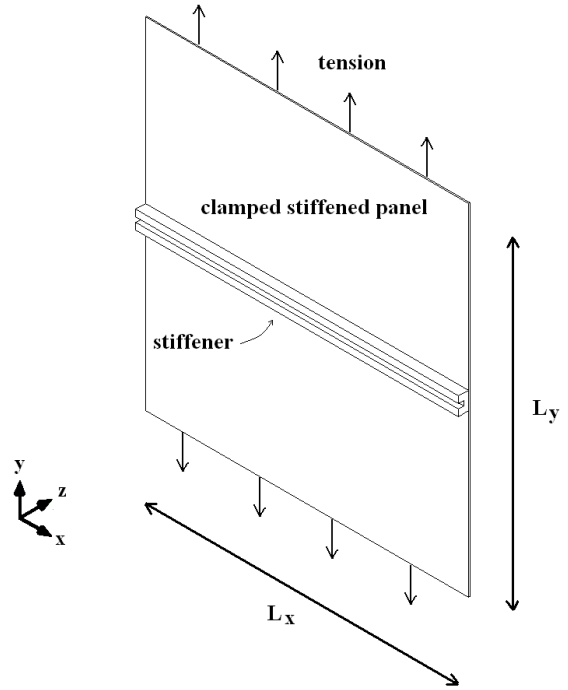

Figure 1: Diagram of the tensioned, stiffened panel.

to generate the structural mass and stiffness matrices and to determine the eigenproperties of the first 60 modes of the panel. The first nine modes of the stiffened panel are shown in Figure 2. Notice that the model includes both global and local modes. The local modes are a result of the size difference between the two bays.

The investigation presented here is limited to piezoceramic actuators and ideal point velocity sensors. While the mass of the sensors is neglected, the dynamics of the piezoelectric actuators are included in the system model as,

$$[M_s + M_p]\,\ddot{\eta} + C_s\dot{\eta} + [K_s + K_p]\,\eta = B_f f + \Theta v \tag{1}$$

where η is a vector of generalized displacements, M_s is the structural mass matrix, M_p is the piezoceramic mass matrix, C_s is the structural damping matrix, K_s is the structural stiffness matrix, K_p is the piezoceramic stiffness matrix, B_f is the forcing matrix, Θ is the electromechanical coupling matrix, f is a vector of structural forces, and v is a vector of applied voltages [1, 10]. For this investigation, we assume proportional damping with a modal damping ratio of 0.01 for all 60 modes included in the model.

Although the structural mass and stiffness matrices could be determined directly from the FE model, the piezoelectric mass, stiffness, and electromechanical coupling matrices had to be calculated using,

$$M_p = \int_{\chi} \Phi^T S_p(\chi)\rho_p\Phi d\chi \tag{2}$$

$$K_p = \int_{\chi} (L_u\Phi)^T S_p(\chi)\kappa_p(L_u\Phi)d\chi \tag{3}$$

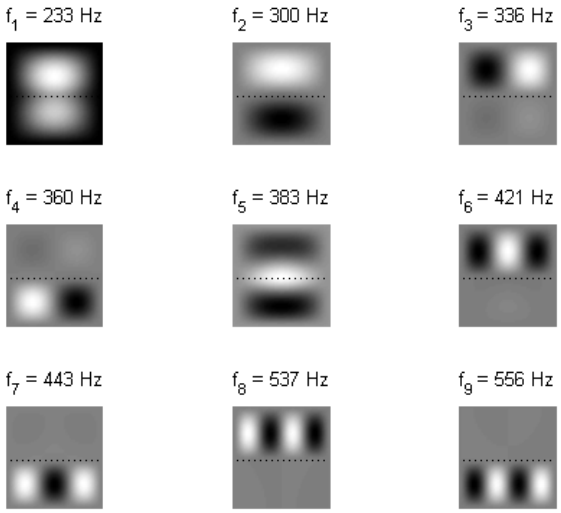

Figure 2: Mode shapes for the first nine modes of the panel.

$$\Theta = \int_{\chi} (L_u \Phi)^T S_p(\chi) e^T (L_\phi \Phi) d\chi \tag{4}$$

where χ is the domain of the structure, Φ are the eigenfunctions of the structure, S_p is the spatial aperture of the transducer, ρ_p is the density of the piezoelectric material, L_u is the elastic differential operator, κ_p is the flexural stiffness of the piezoelectric element, e is a matrix of piezoelectric material constants, and L_ϕ is the electrical differential operator [1, 10]. Each equation was solved numerically using the eigenfunctions obtained from the normal modes analysis.

The dynamic equations for the piezostructure can be rewritten in state-variable form as,

$$\begin{aligned} \ddot{x} &= Ax + Bu \\ y &= Cx + Du \end{aligned} \tag{5}$$

where

$$x(t) = \begin{bmatrix} \eta(t) \\ \dot{\eta(t)} \end{bmatrix}, \quad u(t) = \begin{bmatrix} f \\ v \end{bmatrix}, \tag{6}$$

$$A = \begin{bmatrix} 0 & I \\ -M^{-1}K & -M^{-1}C_s \end{bmatrix}, \quad B = \begin{bmatrix} 0 & 0 \\ M^{-1}B_f & M^{-1}\Theta \end{bmatrix}, \tag{7}$$

$$C = \begin{bmatrix} 0 & \Phi \end{bmatrix}, \quad D = [0], \tag{8}$$

and

$$M = M_s + M_p, \quad K = K_s + K_p. \tag{9}$$

Note that the C matrix is defined such that the output of the system is velocity. The sound power radiated by the structure is calculated using a discrete representation of Rayleigh's integral, as described by Gibbs et al. [20]. The final structural-acoustic model contains 138 states, which includes 60 structural modes and 6 radiation modes. While an excitation filter describing the turbulent boundary layer pressure field could be combined with the structural-acoustic model discussed above, this additional step would not add much value to the analysis. Therefore, a spatially uncorrelated disturbance is used despite the fact that it couples to a plate differently than a turbulent boundary layer excitation [21]. In this study, the uncorrelated disturbance is modeled using 50 uniformly distributed random point loads with unit amplitude. These random point forces are included in the vector f, shown in Equation 1.

3 RESULTS AND DISCUSSION

Three types of control approaches are investigated numerically using the stiffened panel discussed in the previous section: HAC, LAC, and a combined HAC/LAC approach.

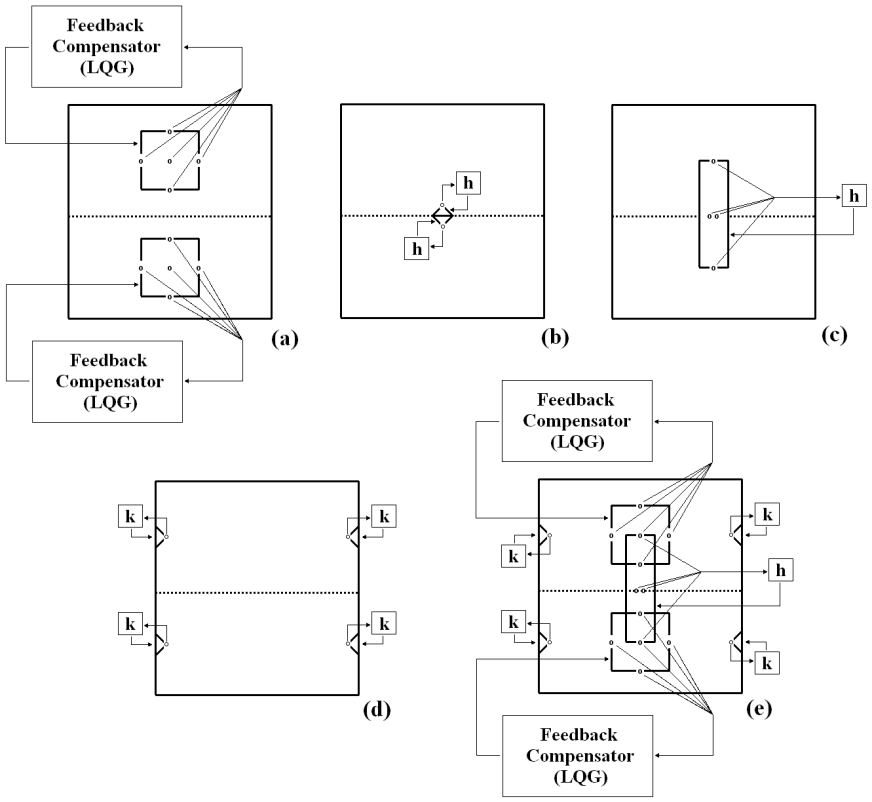

Figure 3: Actuator/sensor configurations and control architectures.

3.1 HAC: Linear quadratic Gaussian control

The simulated results presented in this section are created using decentralized LQG controllers with the HAC configuration shown in Figure 3(a). The transducers consist of a center mounted $0.145\,\mathrm{m} \times 0.145\,\mathrm{m}$ piezoceramic actuator and five point velocity sensors on each bay. The outputs of the five velocity sensors, shown with circles in Figure 3, are

summed together and treated as a single sensor. Gibbs et al. [12] have shown that this type of transducer configuration provides a good tradeoff between controller complexity and performance for a single bay design.

LQG control is an optimal control strategy for systems with process and measurement noise. The controller combines a minimum variance state estimate with an optimal regulator. In general, the LQG design is based on two parameters, β, the frequency-independent control effort penalty, and α, the ratio of measurement to process noise. A control effort penalty of 10^{-6} is used for all of the simulations presented in this work. To determine α, we assume that the process noise enters coincident with the actuator and generates the sensor response. The amplitude of the frequency response function (FRF) between the actuator and sensors on one of the bays can then be used to determine a reasonable value for α. Figure 4 shows the sensor response for one of the bays along with two different measurement noise levels. Since the Kalman estimator is designed with the assumption that only the sensor response above the measurement noise is due to the plant model, the state estimates in the regions where measurement noise dominates the sensor response tend to have low gains [22]. Therefore, increasing the value of α tends to decrease the gain of the state estimates and makes the controller more conservative. The measurement noise levels shown in Figure 4 are $\alpha_i = 10^{-5}$ and $\alpha_{ii} = 10^{-6}$.

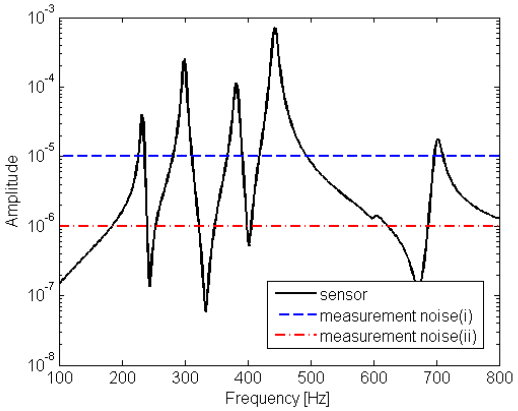

Figure 4: Comparison of process and measurement noise levels.

Figure 5 shows the radiated sound power from a panel excited by an uncorrelated disturbance with unit amplitude. The independent controllers designed with $\alpha_i = 10^{-5}$ achieve a 2.1 dB integrated reduction in the response between 100 and 800 Hz. Reducing α, which tends to make the controller more aggressive, has a negative impact on performance. The controllers designed with $\alpha_i = 10^{-6}$ cause spillover and only achieve an integrated reduction of 1.7 dB. As discussed earlier, the performance of LQG based controllers is limited by the accuracy of the control model. When the plant differs from the control model, inaccurate state estimation can cause spillover of control energy and destabilize the closed-loop system [23]. In this simulation, the bays are structurally coupled and the controllers are designed independently. Therefore, each controller introduces new dynamics that are not included in the control model. As a result, the aggressive control system causes spillover, as shown in Figure 5.

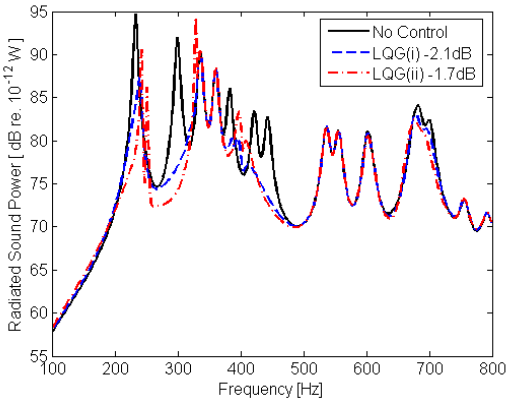

Figure 5: Decentralized LQG control using the actuator/sensor configuration shown in Figure 3(a).

It should be noted that centralized control strategies as well as sequential loop closure techniques can be used to account for the dynamics introduced by neighboring controllers. Unfortunately, centralized strategies are generally not scalable, and sequential loop closure techniques may not be tolerant to actuator or sensor failures.

Despite the interaction between bays, the conservative controller, $\alpha_i = 10^{-5}$, effectively attenuates the 300 Hz, 383 Hz, 421 Hz, and 443 Hz resonances without considerable spillover. Unfortunately, the decentralized LQG control strategy does not adequately reduce the resonance associated with the global mode at 233 Hz. In addition, the HAC system does not target the resonances associated with the third or fourth modes. While these modes do not radiate as efficiently as the first or second structural modes, they still contribute to the total radiated sound power from the panel.

3.2 LAC: Direct output feedback

The LAC systems studied in this paper consist of piezoceramic actuators and point velocity sensors combined with direct output feedback. The transducer configurations are selected to target modes not emphasized by the HAC system. In particular, the LAC systems are designed to target the 233 Hz, 336 Hz, and 360 Hz resonances.

Recently, Gardonio and Elliott [24] have shown that direct output feedback with point sensors and triangular piezoceramic actuators positioned along the edges of a simply supported plate offers good stability bounds. These stability bounds allow high feedback gains, which can be used to add large amounts of damping to the plate. The first LAC configuration studied in this work, shown in Figure 3(b), uses a similar transducer configuration consisting of two actuator/sensor pairs positioned on either side of the stiffener. The goal is to determine whether a triangular actuator and point sensor can be used along the flexible boundary to reduce the amplitude of the 233 Hz resonance.

The frequency response function between one of the actuator/sensor pairs is shown in Figure 6. Since the system is minimum phase only up to 300 Hz, gains that attenuate the 233 Hz resonance cause spillover in the 383 Hz resonance, as shown in Figure 7. These results indicate that the attractive collocation and duality features of the point sensor and

triangular actuator can be lost when the boundary is flexible. This result is not surprising since a triangular actuator produces bending moments along its edges and transverse point forces at the three vertices [25]. If the base of the triangle is positioned along a *rigid* boundary, then the transverse point forces at its base will not couple to the plate, and can therefore be neglected. The point sensor at the vertex opposite of the base edge will then couple to the plate in much the same way as the actuator. If the stiffener is *flexible*, the transverse point forces at the base of the actuator can not be neglected. Therefore the actuator and sensor will not necessarily have good stability bounds, as shown in Figure 6.

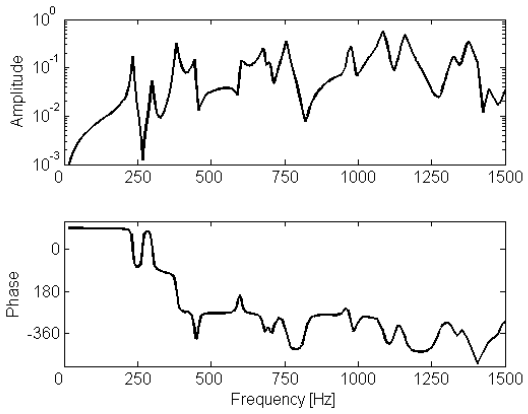

Figure 6: FRF for one of the transducer pairs shown in Figure 3(b)

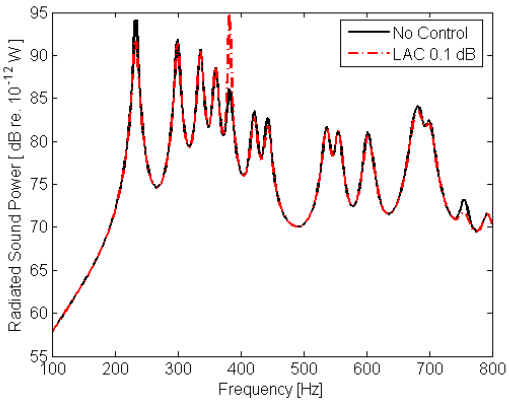

Figure 7: Direct output feedback using the LAC configuration shown in Figure 3(b).

The LAC transducer configuration, shown in Figure 3(c), has good stability bounds despite the flexible boundary. For this configuration, the summed output from four sensors is fed back to control a large rectangular patch that extends across both bays. The frequency response function is passive through 1200 Hz, and emphasizes the first structural mode. The improved stability bounds are due to the size of the actuator and the location of the distributed sensors. As shown in Figure 8, this LAC system reduces the first resonance by 12 dB and achieves a 1.5 dB integrated reduction from 100 to 800 Hz.

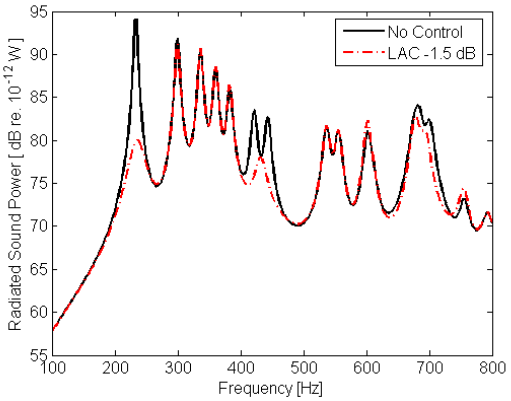

Figure 8: Direct output feedback using the LAC configuration shown in Figure 3(c).

Although the triangular actuator and point sensor are not effective along the stiffener, they can be used on the clamped edges of the panel. This improves the stability bounds of the LAC system since the bending moment and transverse point forces generated at the clamped boundary can be neglected. The frequency response function for one of the transducer pairs, shown in Figure 9, is passive through 1500 Hz.

Due to the stability of this control arrangement, high feedback gains could be used to reduce the amplitude of the panel resonances as shown in Figure 10. With only 4 triangular piezoceramic patches and 4 point sensors, this LAC system attenuates the radiated sound power by 3.4 dB integrated from 100 to 800 Hz. However, these transducer pairs do not efficiently couple to the first or second structural modes.

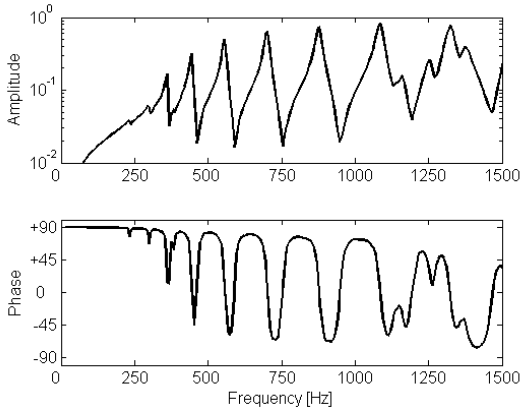

Figure 9: FRF for one of the transducer pairs shown in Figure 3(d).

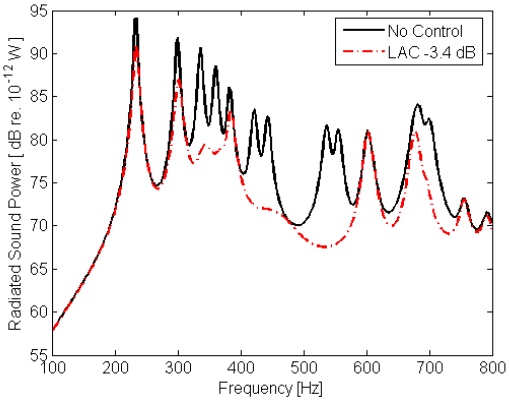

Figure 10: Direct output feedback using the LAC configuration shown in Figure 3(d).

3.3 Combined HAC/LAC approach

Figure 3(e) shows the combined HAC/LAC system, which consists of 8 sensors per bay, with piezoceramic actuators that cover approximately 20% of the surface area and add 7% to the weight of the panel. For these simulations, the LQG controllers are designed using plant responses that are identified after the low-authority feedback loops are closed. In general, the LAC system reduces the amplitude of the resonances. Adding damping to the structure makes the effective plant easier to model and thus improves the computational efficiency of the HAC system. Figure 11 shows the open and closed-loop performance of LAC and HAC/LAC control systems. Combining the LAC systems shown in Figure 3(c) and Figure 3(d), reduces the radiated sound power by 4.6 dB integrated from 100 to 800 Hz. The combined HAC/LAC system reduces the 300 Hz resonance by an additional 10 dB and achieves a 6.1 dB reduction in radiated sound power integrated from 100 to 800 Hz.

Aside from the performance benefits discussed above, a combined HAC/LAC strategy can also be used to take advantage of specific characteristics of the disturbance. For instance, if a correlated reference signal is available, then the decentralized LQG portion

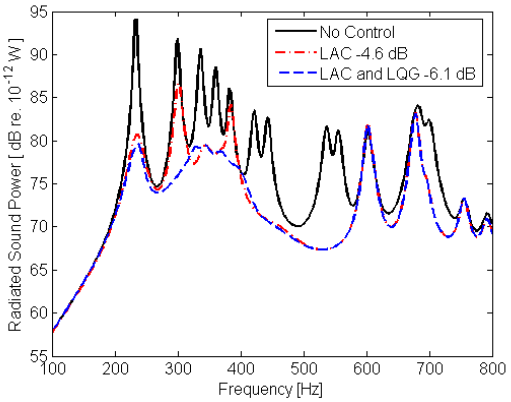

Figure 11: Decentralized LQG and direct output feedback control using the HAC/LAC configuration shown in Figure 3(e).

of the control architecture could be replaced with a hybrid control strategy that combines both feedback and feedforward techniques [1].

4 CONCLUSIONS

This paper presents simulated results for HAC, LAC, and combined HAC/LAC strategies. The HAC system presented in this paper is based on a decentralized LQG approach with a simple actuator/sensor configuration. Unfortunately, the performance of this design is limited by the fidelity of the control model. In addition, since only local information is available to design the controller, the global (multiple-bay) modes are not targeted by the control system.

The LAC approach addresses the limitations of this particular HAC system. Specifically, robust active damping is used to improve the overall system performance by coupling to modes not emphasized by the HAC design. Direct output feedback is used along the shared boundary to attenuate the resonance associated with the low frequency global mode. This is implemented using a large rectangular piezoceramic actuator and the summed output of 4 velocity sensors. This actuator/sensor pair has good stability margins and effectively attenuates the resonance associated with the first structural mode.

The transducer configuration presented by Gardonio and Elliott [24] consisting of triangularly shaped piezoceramic patches and point velocity sensors appears to be particularly well suited for a combined HAC/LAC control system. Grouping the actuator/sensor pairs along the boundaries of the panel achieves robust active damping without interfering with the HAC transducers in the center of each bay. Simulated results indicate that this transducer configuration does not work well along a flexible boundary such as the stiffener, but is very effective if the boundaries are rigid.

The combined HAC/LAC system achieves good performance with relatively few actuators and sensors. Simulated results indicate sound power reductions of 15 dB at the dominant 233 Hz resonance and more than 6 dB integrated from 100 to 800 Hz.

Although the HAC strategy presented in this work is based on a decentralized LQG approach, in general, it could be selected based on the characteristics of the disturbance.

If, for instance, a partially correlated and causal reference signal is available, then a hybrid control strategy could be implemented along with the LAC design. This will be the focus of future work.

5 ACKNOWLEDGEMENTS

The authors gratefully acknowledge the support of NASA Langley Research Center's Structural Acoustics Branch and the National Institute of Aerospace.

REFERENCES

[1] R. L. Clark, W. R. Saunders, and G. P. Gibbs, *Adaptive Structures, Dynamics and Control* (John Wiley and Sons, NY, 1998).

[2] S. J. Elliott, P. Gardonio, T. C. Sors, and M. J. Brennan, Active vibroacoustic control with multiple local feedback loops, J. Acoust. Soc. Am., **111**(2), 908–915 (2002).

[3] M. J. Balas, Direct velocity feedback control of large space structures, J. Guid. Contr., **2**(3), 252–253 (1979).

[4] B. Petitjean and I. Legrain, Feedback controllers for active vibration suppression, J. Struct. Control, **3**, 111–127 (1996).

[5] B. Petitjean, I. Legrain, F. Simon, and S. Pauzin, Active control experiments for acoustic radiation reduction of a sandwich panel: feedback and feedforward investigations, J. Sound Vib., **252**(1), 19–36 (2002).

[6] E. Bianchi, P. Gardonio, and S. J. Elliott, Smart panel with multiple decentralized units for the control of sound transmission. Part III: control system implementation, J. Sound Vib., **274**, 215–232 (2004).

[7] J. N. Aubrun, Theory of the control of structures by low-authority controllers, J. Guid. Contr., **3**(5), 444–451 (1980).

[8] R. L. Clark and D. E. Cox, Multi-variable structural acoustic control with static compensation, J. Acoust. Soc. Am., **102**(5), 2747–2756 (1997).

[9] J. C. Doyle, Guaranteed margins for LQG regulators, IEEE Trans. Automat. Contr., **AC-23**(4), 756–757 (1978).

[10] J. S. Vipperman and R. L. Clark, Implications of using colocated strain-based transducers for output active structural acoustic control, J. Acoust. Soc. Am., **106**(3), 1392–1399 (1999).

[11] G. P. Gibbs, K. W. Eure, and J. W. Lloyd, Active control of turbulent boundary layer induced sound radiation from aircraft style panels, *Proceedings of Active-99, Ft. Lauderdale, Florida, Dec.* (1999).

[12] G. P. Gibbs, R. H. Cabell, and J. Juang, Controller complexity for active control of turbulent boundary layer noise from panels, AIAA Journal, **42**(7), 1314–1320 (2004).

[13] G. P. Gibbs and R. H. Cabell, Simultaneous active control of turbulent boundary layer induced sound radiation from multiple aircraft panels, *8th AIAA/CEAS Aeroacoustics Conference, Breckenridge, CO., June 17-19*, vol. AIAA 2002-2496 (2002).

[14] J. N. Aubrun and M. J. Ratner, Structural control for a circular plate, J. Guid., Contr., Dynam., **7**(5), 535–545 (1984).

[15] T. Williams, Transmission zersos and high-authority/low-authority control of flexible space structures, J. Guid., Contr., Dynam., **17**(1), 170–174 (1994).

[16] D. C. Hyland, J. L. Junkins, and R. W. Longman, Active control technology for large space structures, J. Guid., Contr., Dynam., **16**(5), 801–821 (1993).

[17] J. M. Montgomery, Modeling of aircraft structural-acoustic response to complex sources using coupled FEM-BEM analyses, *10th AIAA/CEAS Aeroacoustics Conference, Manchester, United Kingdom, May 10-12*, vol. AIAA 2004-2822 (2004).

[18] Y. K. Lin, A brief survey of transfer matrix techniques with special reference to the analysis of aircraft panels, J. Sound Vib. (1969).

[19] M. T. Chang and R. Vaicaitis, Noise transmission into semicylindrical enclosures through discretely stiffened curved panels, J. Sound Vib. (1982).

[20] G. P. Gibbs, R. L. Clark, D. E. Cox, and J. S. Vipperman, Radiation modal expansion: Application to active structural acoustic control, J. Acoust. Soc. Am., **107**(1), 332–339 (2000).

[21] C. Maury, P. Gardonio, and S. J. Elliott, A wave number approach to modelling the response of a randomly excited panel, Part I: General theory and Part II: Application to aircraft panels excited by a turbulent boundary layer, J. Sound Vib., **252**(1), 83–113 and 115–139 (2002).

[22] R. H. Cabell, M. A. Kegerise, D. E. Cox, and G. P. Gibbs, Experimental feedback control of flow induced cavity tones, *8th AIAA/CEAS Aeroacoustics Connference and Exhibit, Breckenridge, Colorado, June 17-19*, vol. AIAA 2002-2497 (2002).

[23] B. Anderson and J. Moore, *Optimal Control: Linear Quadratic Methods* (Prentice Hall, 1990).

[24] P. Gardonio and S. J. Elliott, Smart panels with velocity feedback control systems using triangularly shaped strain actuators, J. Acoust. Soc. Am., **117**(4), 2046–2064 (2005).

[25] J. M. Sullivan, J. E. Hubbard, and S. E. Burke, Modeling approach for two-dimensional distributed transducers of arbitrarty spatial distribution, J. Acoust. Soc. Am., **99**(5), 2965–2974 (1996).